A Statistical Approach to Defining Coffee Management Zones: Integrating Apparent Soil Electrical Conductivity, Altimetry and Satellite Indices for Moisture Monitoring

Eduardo Antonio Speranza[1], Ednaldo José Ferreira[2], Luis Henrique Bassoi[2], Ladislau Marcelino Rabello[2], Carlos Manoel Pedro Vaz[2], André Torre Neto[2]

[1]Brazilian Agricultural Research Corporation (Embrapa Digital Agriculture), Campinas, SP, Brazil.

[2]Brazilian Agricultural Research Corporation (Embrapa Instrumentation), São Carlos, SP, Brazil.

A paper from the Proceedings of the

17th International Conference on Precision Agriculture and 11th Brazilian Congress on Precision and Digital Agriculture

13-15 July 2026

Porto Alegre, Brazil

Abstract.

Precision agriculture increasingly relies on spatial data to optimize crop management; however, delineating accurate Management Zones (MZs) in perennial crops like coffee (Coffea arabica L.*) presents unique challenges. Optical remote sensing alone primarily captures transient canopy-surface conditions, which often fail to reflect deeper agronomic realities. To address this limitation, this study evaluated the improvements in MZ delineation achieved by integrating a robust four-year time series of high-resolution multispectral imagery with soil and topographic attributes. The objective was to establish a spatial framework tailored for practical agronomic interventions, specifically optimizing regionalized soil moisture monitoring and selective harvesting strategies. The research was conducted across two commercial coffee fields in São Carlos, state of São Paulo, Brazil. To capture a comprehensive environmental profile, the dataset combined high-frequency three-meter spatial resolution multi-spectral images from SuperDove® nanosatellites with precise in-field measurements of apparent soil electrical conductivity (ECa) and high-precision GNSS altimetry. Following spatial standardization via geostatistical interpolations, a Variance Inflation Factor (VIF) multicollinearity analysis eliminated redundant variables. MZs were delineated employing Ward's hierarchical clustering. The optimal number of zones and attribute influences were validated using a Variance Reduction (VR) metric derived from historical Sentinel-2 NDVI data and ANOVA F-statistics. The VIF analysis successfully streamlined the dataset from fourteen down to five essential attributes per field: ECa, altimetry, and crucial spectral bands and vegetation indices. The VR metric confirmed that a two-zone (2-MZ) configuration was the optimal spatial arrangement, achieving substantial within-zone variance reductions of approximately 60% and 80%. Furthermore, F-statistics highlighted that altimetry and ECa possessed the highest separating power for subdividing the fields, exerting a stronger influence on cluster formation than historical canopy reflectance alone. In conclusion, fusing time-series optical data with soil and terrain attributes fundamentally enhances the reliability of MZs in coffee cultivation. Because altimetry dictates water runoff and ECa reflects localized soil texture and water capacity, these MZs establish an accurate operational framework for regionalized soil moisture monitoring. This multi-source approach empowers farmers to confidently implement site-specific water*

The authors are solely responsible for the content of this paper, which is not a refereed publication. Citation of this work should state that it is from the Proceedings of the 17th International Conference on Precision Agriculture and 11th Brazilian Congress on Precision and Digital Agriculture. EXAMPLE: Last Name, A. B. & Coauthor, C. D. (2026). Title of paper. In Proceedings of the 17th International Conference on Precision Agriculture and 11th Brazilian Congress on Precision and Digital Agriculture (unpaginated, online). Monticello, IL: International Society of Precision Agriculture and Brazilian Congress on Precision and Digital Agriculture.

management and selective harvesting, supporting crop resilience and optimizing resource allocation.

Keywords.
Remote sensing, proximal sensing, spatiotemporal analysis.

Introduction

The characterization of the spatiotemporal behavior of soil and plant attributes represents the elementary step toward the adoption of precision agriculture (PA). The expanding availability of multi-temporal remote sensing imagery with enhanced spatial resolution has rendered the delineation of management zones (MZs) an increasingly feasible strategy (Javadi et al., 2022; Maia et al., 2023). By mapping the spatiotemporal variability of crop parameters, farmers can transition from uniform field management to site-specific interventions based on PA concepts. MZs allow for spatially differentiated interventions that consider vegetative vigor throughout the crop cycle or plant yield. For complex perennial crops like coffee (*Coffea arabica* L.), this type of zoning can be an important tool for the farmer towards starting crop management based on PA, enabling them to address landscape heterogeneity and optimize production (Martello et al., 2022).

Recent advances in orbital platforms have significantly encouraged the use of remote sensing in coffee cultivation. Studies frequently highlight the efficacy of vegetation indices (VI) derived from high-resolution satellites in monitoring crop phenology, biomass accumulation, and yield potential (Vaz et al., 2025). Time-series analyses of multi-spectral imagery are increasingly employed to map canopy vigor and evaluate field performance across varying environmental conditions (Vasconcelos et al., 2025). For instance, Chedid et al. (2024) demonstrated the analytical potential of multi-spectral images provided by nanosatellites to identify the best vegetation indices for monitoring the coffee growing season. These indices can successfully delineate zones of distinct yield potential, providing a robust historical dataset that reflects the cumulative effects of climate and field management to guide site-specific agronomic interventions.

However, while optical remote sensing provides a comprehensive view of the crop's vegetative state, it is inherently limited to the surface of the canopy. In perennial systems, relying exclusively on canopy metrics overlooks critical sub-surface variations. When the goal is to implement interventions based on specific soil characteristics, remote sensing exhibits certain limitations. Consequently, recent studies have chosen the integration of proximal soil sensing and soil sampling to achieve a balanced characterization. Silva et al. (2024) highlighted this need by using a set of soil chemical variables extracted from soil samples at different depths, coupled with geostatistical tools, to define MZs of a coffee crop, presenting a flexible alternative to machine learning approaches. The measurement of apparent soil electrical conductivity (ECa) via electromagnetic induction instruments has also emerged as a highly effective technique, providing a continuous, non-invasive assessment of the soil profile that reveals underlying spatial patterns directly influencing root development (Gonçalves et al., 2025).

In Brazil, the world's largest coffee producer and exporter (ICO, 2026; USDA, 2025), the states of Minas Gerais, São Paulo, and Espírito Santo are responsible for the majority of production, characterized by a high diversity of microclimates, altitudes, and soil types, which directly influence crop development and beverage quality (Parreiras et al., 2025). The topographic complexity of coffee-growing landscapes in these regions further guides the need for multi-source data integration in order to identify spatial variability with greater precision. Addressing this, Silva et al. (2025) developed a cell-size approach to deal with the spatial and temporal variability management of coffee crops, based on soil fertility and historical yield. Furthermore, incorporating yield and maturity metrics is crucial for finalizing management strategies. Kazama et al. (2021) successfully defined MZs for a coffee crop field based on the yield and maturity of pre-harvested samples to guide full harvesting by agricultural machinery. By fusing multi-temporal canopy data with stable soil, terrain, and yield attributes, it is possible to delineate MZs that encapsulate the holistic underlying soil-plant relationships.

Addressing this need for multi-source data integration, previous research conducted on two *Coffea arabica* L. production fields in São Carlos, state of São Paulo, Brazil, delineated MZs based solely on historical remote sensing-derived vegetation indices (VI) from Planet nanosatellites and Sentinel-2 (Speranza et al., 2025). While that foundational study successfully utilized clustering algorithms and non-parametric statistical tests to establish MZs for biomass-related management and identified promising areas for high-quality coffee production, it relied entirely on canopy reflectance. Building on that initial effort, the current study sought to quantify the improvements resulting from the inclusion of additional soil and terrain attributes. To achieve that purpose, the MZs were re-delineated using hierarchical clustering algorithms on an expanded dataset integrating historical remote sensing vegetative vigor data, ECa and high-precision GNSS altimetry. By comparing the MZs obtained from this multi-source approach to those derived from remote sensing data alone, this study aims to assess the gains in spatial variability representation and practical utility, such as regionalized soil moisture monitoring and selective grain harvesting for identifying higher and lower quality beverages at the end of the process.

Materials and Methods

Study Area and Data Acquisition

The study was conducted in the municipality of São Carlos, São Paulo, Brazil (22°00'55" S, 47°53'28" W), at an elevation of 856 m above sea level. Two *Coffee arabica* L. sites were analyzed: field 1 (F01), with an area of 2.5 ha, altitude from 865 m to 894 m, and with the cv. Catuai Vermelho planted in 2016; and field 2 (F02), with an area of 3.5 ha, altitude from 863 to 893 m, and with the cv. Catuai Amarelo planted in 2018.

Multi-spectral satellite images composed by 8 bands (Coastal Blue, Blue, Green I, Green II, Yellow, Red, Red Edge and Near-Infrared) with wavelengths ranging from 431 to 885 nm, spatial resolution of 3 m and daily revisit were obtained from the SuperDove® sensor (PSB.SD) (Planet Team, 2026), provided by RedeMAIS/MJSP, regarding the four previous crop seasons (from 2021-2022 to 2024-2025). For each crop season, only cloud-free and shadow-cloud-free images in corresponding phenological stages from green pinhead to bean grain (from November to March months) were collected, resulting in a time-series of 25 images for each field. In order to have historical data for each field that would help statistically validate the obtained MZs, average maps of the NDVI vegetation index (Rouse et al., 1973) were generated from the Sentinel-2 satellite (European Space Agency, 2026), considering time series from the studied periods, regarding only cloud-free and shadow-cloud-free images. The source of this data is the Google Earth Engine platform (Gorelick et al., 2017).

ECa data were obtained from a single collection carried out in both fields in November 2025 with the EM-38 MK2® sensor (Geonics Limited, Mississauga, Ontário, Canadá), considering the standard depths of 1.5 m and 0.75 m. Using a high-precision portable GNSS receiver, model TopCon GRS1® (TopCon Positioning Systems, Livermore, California, USA), attached to this equipment, it was possible to obtain altimetry data considering the same grid of points as the ECa values. This data collection was carried out on foot, with data being collected continuously along the crop planting rows.

Data Processing and Attribute Selection

The processing of satellite images was carried out similarly for both studied fields. Initially, the vegetation indexes (VI) NDVI, NDRE, EVI2, and SAVI, widely used in the literature for identifying spatial variability of agricultural crops (Maia et al., 2023; Vera-Esmeraldas et al., 2025), were calculated for all 25 images collected for both fields. This processing was performed using functions of the FieldImageR package (Matias et al., 2020), available for the R software. To account for the temporality of the data and, at the same time, allow integration with ECa and altimetry data collected on a single date, average values of the 12 multi-spectral attributes (4 vegetation indices and 8 bands) were generated for all pixels within fields F01 and F02, resulting in sample grids of 3188 and 4088 pixels, respectively.

In order to integrate the ECa data at both depths and altimetry with the remote sensing data, it was necessary a standardization of the spatial grid for these attributes, based on the original 3 m grid of the images. Therefore, geostatistical procedures such as semivariogram adjustments and spatial interpolations by kriging were performed using the Smart Map plugin (Pereira et al., 2022), available for the QGIS software version 3.42.3. For the ECa analysis, only measurements obtained at a depth of 1.5 m were considered, as the dataset collected at 0.75 m contained more than 10% outliers. These values were identified as outliers because they exhibited extreme negative readings, which are physically inconsistent with the nature of ECa measurements.

Spectral reflectance bands and VIs derived from them typically exhibit high multicollinearity. Thus, multicollinearity analyses were performed considering the variance inflation factor (VIF) values of each one (James et al., 2013) considering the 14 attributes of each original database (4 VIs, 8 spectral bands, ECa and altimetry). Initially, attributes with high multicollinearity (VIF > 5) were eliminated considering the entire set of attributes. Then, the remaining attributes were evaluated one by one, recursively, until only variables with low multicollinearity remained.

Finally, to avoid undesirable effects that could be caused by pixels located on the border, a negative buffer of 3 m was implemented for both plots, considering their respective contours collected in the field with a RTK GNSS receiver model Emlid Reach RS3®. As a result, the number of samples with values for the selected attributes was reduced to 2677 for F01 and 3554 for F02.

Delineation of Management Zones (MZ)

For the delineation of MZs in this study, Ward's hierarchical clustering algorithm (Ward Jr., 1969) was employed. A defining characteristic of Ward's method is its variance-minimizing approach, which sequentially merges clusters to minimize the total within-cluster error sum of squares. Prior to the clustering process, it was necessary to normalize each layer of information to a range between -1 and 1, ensuring that variables with varying magnitudes contributed equally to the distance calculations. Furthermore, a major advantage of using this hierarchical technique is the ability to visually and analytically explore the structural hierarchy of the data, typically by means of a dendrogram, which entirely eliminates the need to predefine the desired number of clusters a priori. Anyway, for experimental purposes, this study considered a minimum of 2 and a maximum of 10 MZs, considering that a very high number of MZs can excessively stratify the field and their design may lose its practical meaning.

Statistical Validation

Regarding predefined number of MZs (from 2 to 10), the variance reduction (VR) metric was used to indicate suitable number of MZs for each field (Schenatto et al., 2017). This metric allows calculating the variance reduction provided by a given number of MZs for a field, considering the geographic area of each MZ proportionally to the whole field area; and choosing a target variable that can represent the spatial variability of the area over time. Due to the lack of historical yield data, an average NDVI map was used as a surrogate indicator of crop performance. This map integrated information from at least four previous seasons and, despite its lower spatial resolution (10 m/pixel) compared with the imagery employed for management zone delineation, provided greater temporal representativeness of crop behavior. The VR metric tends to show higher values as the number of MZs increases, reaching a plateau in this increase at an intermediate number of MZs. To calculate VR for each generated MZ map, a custom R function was developed to compute the area and variance of each MZ and of the entire field.

Finally, to verify the influence of soil, terrain and remote sensing attributes in this process, the F-statistic of the analysis of variance (ANOVA) technique was used to identify the separability power of the attributes for each generated clustering level. In this case, for a given attribute, higher values indicate a greater ability for it to separate clusters at each level. These calculations were performed using the *aov* function from the stats package in R. For this analysis, statistical significance was established at p-value < 0.05.

Results and Discussion

The first result of this study shows the capability of the collected field data related to soil (ECa) and altimetry to contribute in defining the spatial variability of F01 and F02. Fig. 1 shows semivariogram adjustments for all cases, with coefficients of determination (R^2) varying from 0.85 to 0.98, increasing the reliability of kriging-interpolated maps.

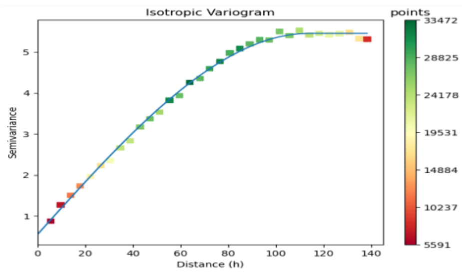

(a)

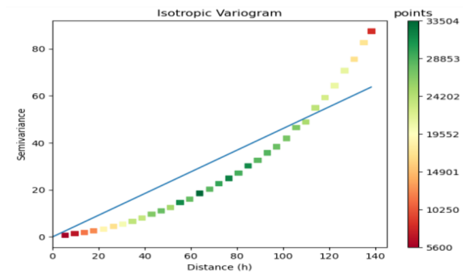

(b)

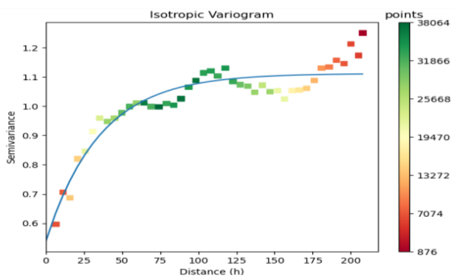

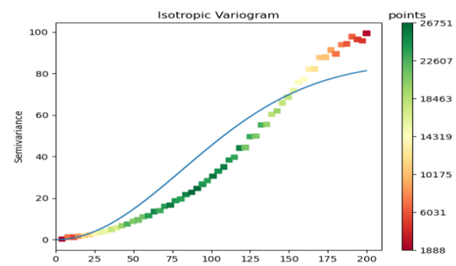

(c) (d)

Fig. 1. Semivariogram adjustments for ECa at 1.5 m depth and altimetry for F01 (a and b) and F02 (c and d), respectively.

From the fitted semivariograms above, ECa and altimetry maps were obtained for F01 and F02 using spatial interpolation by kriging, as described in the previous section. Next, a multicollinearity analysis was performed and resulted in a reduction from 14 to 5 attributes for each dataset. All removed attributes were multispectral bands or VI, demonstrating the high correlation existing between these types of data. It is worth highlighting that the attributes collected in the field (ECa and altimetry) were maintained for both datasets, as well as the Coastal Blue and NIR bands. Fig. 2 shows the Pearson correlation matrix between the remaining attributes for F01 (Fig. 2a) and F02 (Fig. 2b).

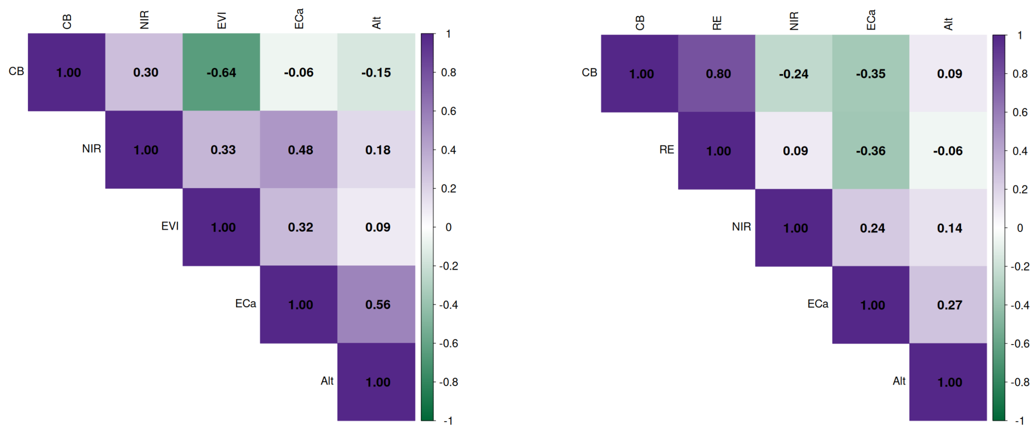

(a) (b)

Fig. 2. Pearson's correlations for the remaining attributes after multicollinearity analysis for F01 (a) and F02 (b), where CB=CoastalBlue, Alt=Altimetry and RE=RedEdge.

The attributes selected for both areas may represent distinct characteristics of soil, plant, atmosphere and terrain which can be important for a more precise identification of the spatial variability of the area as a whole, enhancing its use for delineating MZs. ECa is commonly correlated with textural variations, water availability and, consequently, yield potential (Singh et al., 2016). On the other hand, NIR is closely linked to vegetative vigor, biomass, leaf area index and chlorophyll content of plants, being a fundamental spectral band for calculating VIs such as NDVI (Nogueira et al.,2021; Chemura et al., 2018). Additionally, both the RedEdge band and the EVI have the ability to identify the spatial variability of plants during the end-of-cycle periods, where NDVI and other NIR-based indices face difficulties related to saturation (Tian et al., 2025). The Coastal Blue band also plays an important role in matters related to atmospheric interference, allowing for the correction of the reflectance of other spectral bands with respect to this factor (Tsuchiya et al., 2025). Finally, altimetry data in fields with considerable differences in altitude, such as those found in F01 and F02, can be important to assist in identifying issues related to water runoff and accumulation (Farrell et al., 2023).
Considering the selected attributes and the hierarchical clustering algorithm specified in the previous section, maps containing 2 to 10 potential MZs were generated for each field. Fig. 3 shows graphics with the VR metric results for each MZ potential map, regarding average NDVI values from Sentinel-2 satellite over the last four harvests as the target attribute.

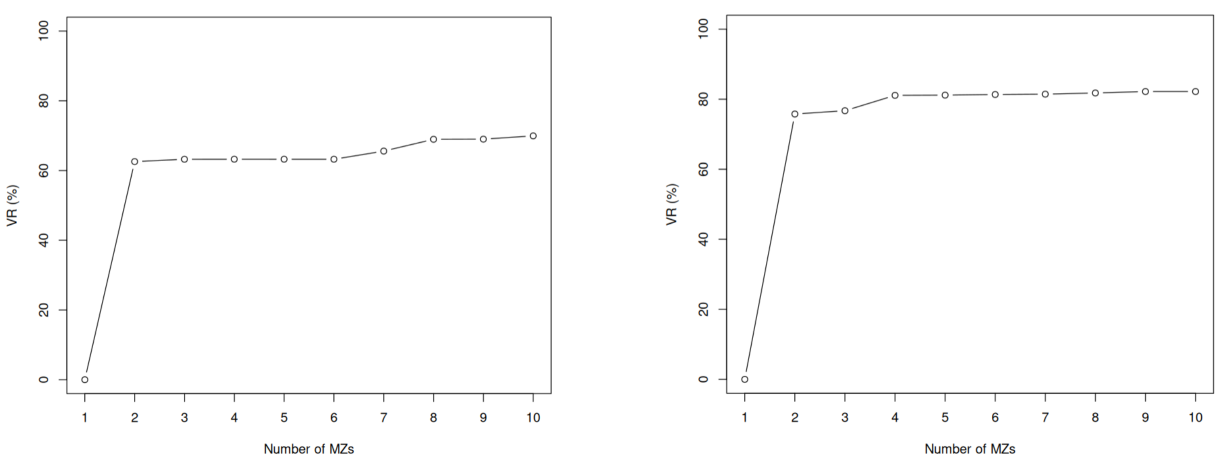

(a) (b)

Fig. 3. VR values obtained for different numbers of MZs for plots F01 (a) and F02 (b).

Regarding the graphs above, it is possible to observe that high VR values were obtained for both areas (about 60% and 80%, respectively), even in the first configuration that considers only two MZs. Based on a VR=0, where the split of the field into MZs is not considered (1 MZ), the attributes used by the clustering algorithm, acting together, indicate that in both fields the MZ delineation should be considered for carrying out spatially differentiated interventions. Also in both cases, it is possible to observe the emergence of a plateau in the graph, that is, a not significant increase in VR starting from 2 MZs. Therefore, the recommended approach would be to use 2 MZs for both fields, which already results in a significant reduction in variance compared to not using MZ, and this can work well in practical terms. Fig. 4 shows the results of the F-statistic for all attributes in all clustering configurations, for both fields. All results were verified and identified with a p-value below 5%.

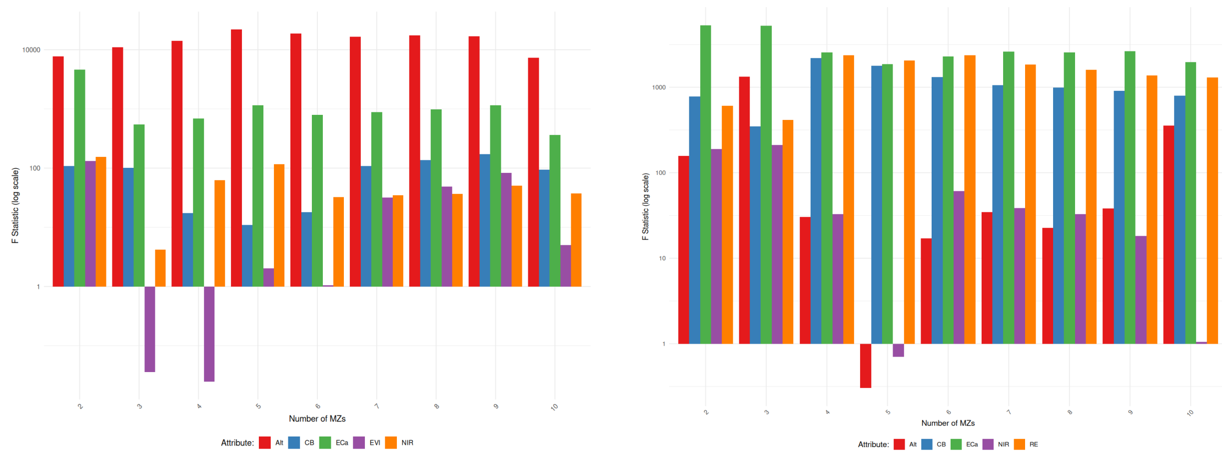

(a) (b)

Fig. 4. F-statistic indicating the separability power of each attribute, for each field, to contribute to the subdivision of MZs for F01 (a) and F02 (b). Alt=Altimetry; CB=Coastal Blue; RE=RedEdge

Regarding the graphs in Fig. 4, it is possible to verify, for F01 (Fig. 4a), that the attribute that most contributes to the subdivision of the field, for all cases, is the altimetry (Alt), followed by the ECa and the spectral band Costal Blue (CB). For F02 (Fig. 4b), ECa, CB and RedEdge (RE) stand out. Fig. 5 shows the maps with 2 MZs for fields F01 and F02, as well as the maps of the attributes mentioned above.

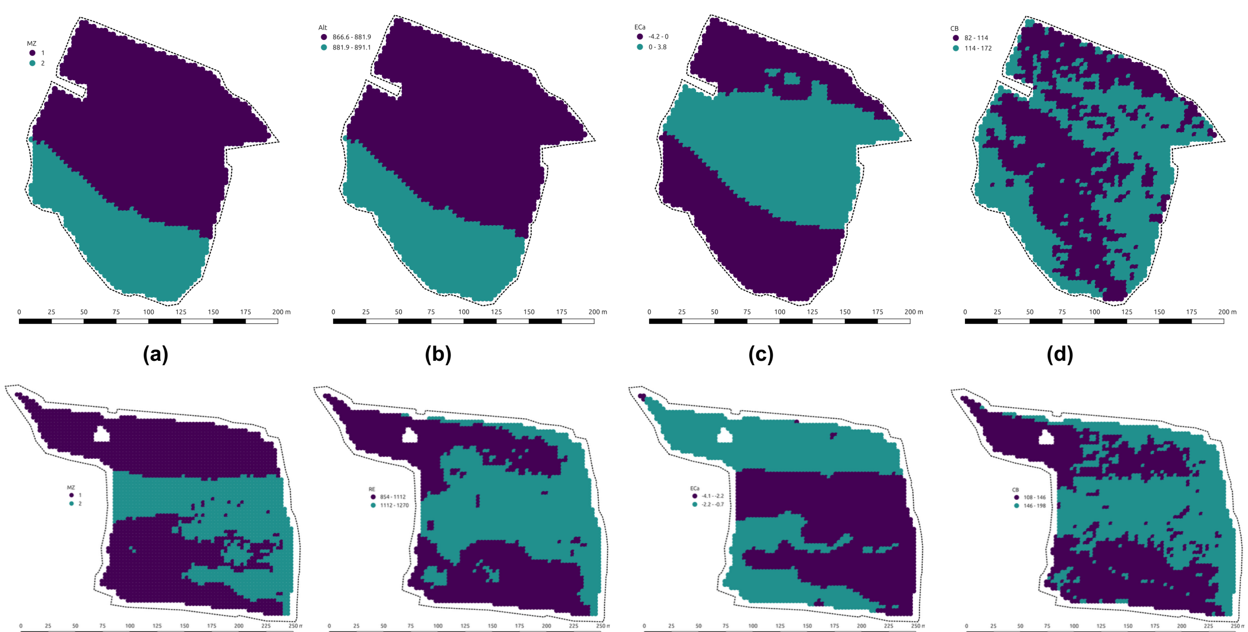

(a) (b) (c) (d)

(e) (f) (g) (h)

Fig. 5. Maps of 2 MZs for F01 (a) and F02 (e) and attribute maps of altimetry (Alt in m) (b), ECa (mS/m) (c) and CoastalBlue (d), for F01; and of ECa (mS/m) (f), CoastalBlue (g) and RedEdge (h) for F02.

Regarding the MZ and attribute maps used for their delineation (Fig. 5), it is possible to visualize similarities in the observed patterns and the influence of each of them on the final MZ map, mainly altimetry and ECa. Table 1 shows numerically the differences in average values for each attribute, considering the MZs individually.

Table 1. Minimum, Maximum, MZ1 and MZ2 average values of the best attributes for F01 and F02 – Alt=Altimetry; CB=Coastal Blue; RE=RedEdge

	F01			F02		
	Alt	**ECa**	**CB**	**ECa**	**CB**	**RE**
Min	866	-4.22	82	-4.09	108	854
Max	891	3.82	172	-0.73	198	1296
MZ1	884	1.17	114	-1.83	143	1093
MZ2	872	-2.22	118	-2.92	153	1127

Observing the data in Table 1, for F01, the Alt attribute shows a 25-meter difference between the extremes of the whole area and an average difference of 12 meters between the two delimited MZs, confirming this attribute as mandatory for defining the 2 MZs. ECa, with a total interval of 8.04 and an average difference of 3.39 between the MZs, also indicates separability potential, confirming the values obtained with the F-statistic (Fig. 4). For F02, ECa has a total range of 3.36, with an average difference of 1.09 between the MZs; however, the differences between MZs for the data originating from remote sensing are proportionally much smaller, also indicating, in agreement with the graphs in Fig. 04, that ECa is mandatory for the variability of F02.

Given this data and analysis, some observations may be relevant for interpreting the results. The ECa and altimetry data are relevant to the establishment and consolidation of MZs. Additionally, unlike remote sensing attributes, these attributes underwent a geostatistical process that, in a way, helps to smooth the final maps, which also favors the delineation of MZs. On the other hand, although remote sensing data are a consolidation of historical average values from four previous harvests, it is possible that anthropogenic actions may be influencing spatial variability. Another issue concerns spatial resolution, which, despite being quite accurate by current standards (3 m), may have many pixels representing variations in both plant and soil characteristics. In future work, we intend to collect suborbital images in the study areas using drones to assist in a more assertive characterization of the remote sensing pixels.

Conclusion

The integration of multi-source data, specifically combining historical orbital remote sensing with proximal soil sensing (ECa) and high-precision altimetry, proved to be a highly effective approach for delineating management zones (MZs) in complex perennial systems like coffee. The results demonstrated that relying solely on canopy reflectance overlooks critical underlying environmental factors. By reducing the dataset through multicollinearity analysis, the study isolated the most impactful variables, successfully minimizing data redundancy. The variance reduction (VR) and F-statistic analyses increased the likelihood that a two-zone configuration represents the most suitable and practical option for both studied fields, although this conclusion remains inferential rather than definitive. Notably, stable topographic and edaphic attributes, particularly altimetry and ECa, emerged as the primary drivers for spatial clustering, underscoring their indispensable role in accurately characterizing field heterogeneity.

From a practical agronomic standpoint, the strong influence of ECa and altimetry in defining these MZs provides a strategic framework specifically optimized for regionalized soil moisture monitoring. Because altimetry dictates water runoff and accumulation, and ECa is intrinsically linked to soil texture and water-holding capacity, the delineated MZs allow farmers to accurately pinpoint MZs with distinct hydrological behaviors. This enables the strategic placement of soil moisture sensors and the implementation of site-specific irrigation or water management practices, helping to mitigate water stress during critical phenological stages and possibly influencing final beverage quality. Moving forward, the incorporation of ultra-high-resolution suborbital imagery via drones will further refine these MZs by minimizing plant-soil pixel mixing, solidifying a robust, multi-layered framework for precision coffee farming.

Acknowledgments

We thank the owners of Sítio Boa Fé and Café Veneziani, in São Carlos, state of São Paulo, Brazil, for making the study area available; and the Brazilian Coffee Research and Development Consortium (ConCafé) and National Council for Scientific and Technological Development (CNPq), Brazil, for funding this research.

References

Chedid, V., Cortez, J. W., & Arcoverde, S. N. (2024). Monitoring the vegetative state of coffee using vegetation indices. Engenharia Agrícola, 44, e20220212.

Chemura, A., Mutanga, O., Odindi, J., & Kutywayo, D. (2018). Mapping spatial variability of foliar nitrogen in coffee (Coffea arabica L.) plantations with multi-spectral Sentinel-2 MSI data. ISPRS Journal of Photogrammetry and Remote Sensing, 138, 1-11.

European Space Agency. (2024). Sentinel-2 MSI Level-2A Surface Reflectance. Copernicus Service Information. (Acesin May 06 2026).

Farrell, M., Leizica, E., Gili, A., & Noellemeyer, E. (2023). Identification of management zones with different potential moisture availability for sustainable intensification of dryland agriculture. Precision Agriculture, 24(3), 1116-1131.

Gonçalves, L. A., de Souza, E. G., Nóbrega, L. H., Bier, V. A., Maggi, M. F., Bazzi, C. L., & Uribe-Opazo, M. A. (2025). Spatial and temporal variability of soil apparent electrical conductivity. Precision Agriculture, 26(1), 10.

Gorelick, N., Hancher, M., Dixon, M., Ilyushchenko, S., Thau, D., & Moore, R. (2017). Google Earth Engine: Planetary-scale geospatial analysis for everyone. Remote Sensing of Environment, 202, 18–27. doi.org.

International Coffee Organization (ICO). (2026, March). *Coffee Market Report*. ico.org.

James, G., Witten, D., Hastie, T., & Tibshirani, R. (2013). An introduction to statistical learning: with applications in R (Vol. 103). New York: springer.

Javadi, S. H., Guerrero, A., & Mouazen, A. M. (2022). Clustering and smoothing pipeline for management zone delineation using proximal and remote sensing. *Sensors*, *22*(2), 645.

Kazama, E. H., da Silva, R. P., Tavares, T. D. O., Correa, L. N., de Lima Estevam, F. N., Nicolau, F. E. D. A., & Maldonado Júnior, W. (2021). Methodology for selective coffee harvesting in management zones of yield and maturation. Precision Agriculture, 22(3), 711-733.

Maia, F. C.O., Bufon, V. B., & Leão, T. P. (2023). Vegetation indices as a tool for mapping sugarcane management zones. Precision Agriculture, 24(1), 213-234.

Martello, M., Molin, J. P., Wei, M. C. F., Canal Filho, R., & Nicoletti, J. V. M. (2022). Coffee-Yield Estimation Using High-Resolution Time-Series Satellite Images and Machine Learning. AgriEngineering, 4(4), 888-902. https://doi.org/10.3390/agriengineering4040057

Matias, F. I., Caraza-Harter, M. V., & Endelman, J. B. (2020). FIELDimageR: An R package to analyze orthomosaic images from agricultural field trials. The Plant Phenome Journal, 3(1), e20005.

Parreiras, T. C., Santos, C. d. O., Bolfe, É. L., Sano, E. E., Leandro, V. B. S., Bayma, G., Silva, L. A. P. d., Furuya, D. E. G., Romani, L. A. S., & Morton, D. (2025). Dense Time Series of Harmonized Landsat Sentinel-2 and Ensemble Machine Learning to Map Coffee Production Stages. *Remote Sensing*, *17*(18), 3168. https://doi.org/10.3390/rs17183168.

Pereira, G. W., Valente, D. S. M., Queiroz, D. M. D., Coelho, A. L. D. F., Costa, M. M., &

Grift, T. (2022). Smart-map: an open-source QGIS plugin for digital mapping using machine learning techniques and ordinary kriging. Agronomy, 12(6), 1350.

Planet Team. (2024). Planet Application Program Interface: PlanetScope SuperDove (PSB.SD). Planet Labs PBC. https://www.planet.com/ (Acess in May 06 2026).

Silva, C. D. O. F., Grego, C. R., Manzione, R. L., Oliveira, S. R. D. M., Rodrigues, G. C., Rodrigues, C. A. G., ... & Koenigkan, L. V. (2024). Summarizing soil chemical variables into homogeneous management zones–case study in a specialty coffee crop. Smart Agricultural Technology, 7, 100418.

Silva, E. R. O. d., Silva, T. L. d., Wei, M. C. F., Souza, R. A. d., & Molin, J. P. (2025). Spatial and Temporal Variability Management for All Farmers: A Cell-Size Approach to Enhance Coffee Yields and Optimize Inputs. *Plants*, *14*(2), 169. https://doi.org/10.3390/plants14020169

Schenatto, K., De Souza, E. G., Bazzi, C. L., Gavioli, A., Betzek, N. M., & Beneduzzi, H. M. (2017). Normalization of data for delineating management zones. Computers and Electronics in Agriculture, 143, 238-248.

Singh, G., Williard, K. W., & Schoonover, J. E. (2016). Spatial relation of apparent soil electrical conductivity with crop yields and soil properties at different topographic positions in a small agricultural watershed. Agronomy, 6(4), 57.

Speranza, E. A, Ferreira, E., Bassoi, L.H. (2025). Mapping coffee management zones using satellite-derived indices and clustering-based methods: a statistical differentiation approach. In: SIMPÓSIO NACIONAL DE INSTRUMENTAÇÃO AGROPECUÁRIA, 5., 2025, São Carlos. Anais [...]. São Carlos: Embrapa Instrumentação, 2025. p. 639-643.

Tian, Z., Fan, J., Yu, T., de Leon, N., Kaeppler, S. M., & Zhang, Z. (2025). Mitigating NDVI saturation in imagery of dense and healthy vegetation. ISPRS Journal of Photogrammetry and Remote Sensing, 227, 234-250.

Tsuchiya, Y., & Sonobe, R. (2025). Temporal deep learning for multi-crop classification in Hokkaido, Japan using multi-temporal SuperDove imagery. Geocarto International, 40(1), 2596969.

U.S. Department of Agriculture (USDA). (2025). *Coffee: World Markets and Trade*. Foreign Agricultural Service. usda.gov.

Vasconcelos, J. C. S., Arantes, C. S., Speranza, E. A., Antunes, J. F. G., Barbosa, L. A. F., & Cançado, G. M. D. A. (2025). Predicting sugarcane yield through temporal analysis of satellite imagery during the growth phase. Agronomy, 15(4), 793

Vaz, C. M. P., Ferreira, E. J., Speranza, E. A., Franchini, J. C., Naime, J. D. M., Inamasu, R. Y., ... & Galbieri, R. (2025). Cotton Yield Map Prediction Using Sentinel-2 Satellite Imagery in the Brazilian Cerrado Production System. AgriEngineering, 7(11), 390.

Vera-Esmeraldas, A., Pizarro-Oteíza, S., Labbé, M., Rojo, F., & Salazar, F. (2025). UAV-Based Spectral and Thermal Indices in Precision Viticulture: A Review of NDVI, NDRE, SAVI, GNDVI, and CWSI. Agronomy, 15(11), 2569.

Ward, J. H., Jr. (1963). Hierarchical grouping to optimize an objective function. *Journal of the American Statistical Association*, *58*(301), 236–244.